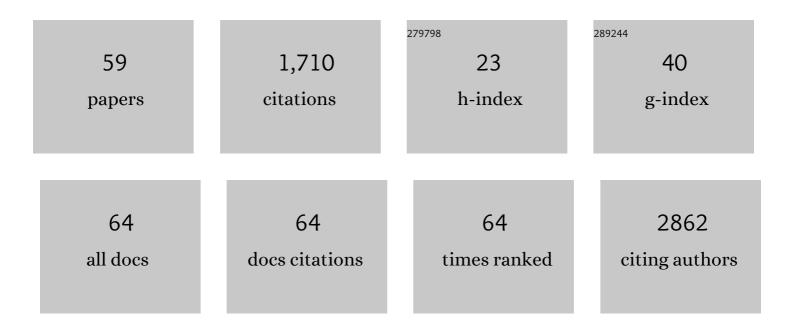
List of Publications by Year in descending order

Source: https://exaly.com/author-pdf/553873/publications.pdf Version: 2024-02-01



ΙΠΠΕ ΛΗΤΑΝΟΛΑ

#	Article	IF	CITATIONS
1	Fabric Investigation of Natural Sensitive Clay from 3D Nano- and Microtomography Data. Journal of Engineering Mechanics - ASCE, 2022, 148, .	2.9	0
2	Assessing implications of nanoplastics exposure to plants with advanced nanometrology techniques. Journal of Hazardous Materials, 2022, 430, 128356.	12.4	20
3	Detection and Characterization of TiO2 Nanomaterials in Sludge from Wastewater Treatment Plants of Chihuahua State, Mexico. Nanomaterials, 2022, 12, 744.	4.1	3
4	Evaluation of imaging setups for quantitative phase contrast nanoCT of mineralized biomaterials. Journal of Synchrotron Radiation, 2022, 29, 843-852.	2.4	8
5	Impact of the growth strategy and device fabrication on the alloy homogeneity in optoelectronic grade Sn-rich GeSn. Materials Science and Engineering B: Solid-State Materials for Advanced Technology, 2021, 264, 114899.	3.5	4
6	Structural and chemical variations in Mg-calcite skeletal segments of coralline red algae lead to improved crack resistance. Acta Biomaterialia, 2021, 130, 362-373.	8.3	6
7	3D Quantification of Microstructural Properties of LiNi <sub>0.5</sub> Mn <sub>0.3</sub> Co <sub>0.2</sub> O <sub>2</sub> Highâ€Energy Density Electrodes by Xâ€Ray Holographic Nanoâ€Tomography. Advanced Energy Materials, 2021, 11, 2003529.	19.5	34
8	X-ray nano-tomography of complete scales from the ultra-white beetles Lepidiota stigma and Cyphochilus. Scientific Data, 2020, 7, 163.	5.3	4
9	<i>Medicago truncatula</i> Ferroportin2 mediates iron import into nodule symbiosomes. New Phytologist, 2020, 228, 194-209.	7.3	23
10	Monitoring the morphological changes of Si-based electrodes by X-ray computed tomography: A 4D-multiscale approach. Nano Energy, 2020, 74, 104848.	16.0	20
11	In situ investigation of atmospheric plasma-sprayed Mn–Co–Fe–O by synchrotron X-ray nano-tomography. Journal of Materials Science, 2020, 55, 12725-12736.	3.7	7
12	Helical Microstructures of the Mineralized Coralline Red Algae Determine Their Mechanical Properties. Advanced Science, 2020, 7, 2000108.	11.2	11
13	Energy and Environmental Science at ESRF. Synchrotron Radiation News, 2020, 33, 40-51.	0.8	3
14	Boosting spatial resolution by incorporating periodic boundary conditions into single-distance hard-x-ray phase retrieval. Journal of Optics (United Kingdom), 2020, 22, 115607.	2.2	10
15	A helium mini-cryostat for the nanoprobe beamline ID16B at ESRF: characteristics and performance. Journal of Synchrotron Radiation, 2020, 27, 1074-1079.	2.4	6
16	High Resolution 3D and 4D Characterization of Microstructure Formation in Novel Ti Alloys for Additive Manufacturing. Microscopy and Microanalysis, 2019, 25, 384-385.	0.4	2
17	Analysis of diatoms by holotomography. Surfaces and Interfaces, 2019, 17, 100358.	3.0	2
18	From spinodal decomposition to alternating layered structure within single crystals of biogenic magnesium calcite. Nature Communications, 2019, 10, 4559.	12.8	36

#	Article	IF	CITATIONS
19	Distribution of nickel and chromium containing particles from tattoo needle wear in humans and its possible impact on allergic reactions. Particle and Fibre Toxicology, 2019, 16, 33.	6.2	48
20	Liquid–liquid phase separation morphologies in ultra-white beetle scales and a synthetic equivalent. Communications Chemistry, 2019, 2, .	4.5	28
21	X-ray fluorescence nano-imaging of long-term operated solid oxide electrolysis cells. Journal of Power Sources, 2019, 421, 100-108.	7.8	13
22	3D visualisation of hepatitis B vaccine in the oral delivery vehicle SBA-15. Scientific Reports, 2019, 9, 6106.	3.3	13
23	Dynamics of the Morphological Degradation of Siâ€Based Anodes for Liâ€Ion Batteries Characterized by In Situ Synchrotron Xâ€Ray Tomography. Advanced Energy Materials, 2019, 9, 1803947.	19.5	59
24	In situ nanotomography study of creep cavities in Al-3.6-Cu alloy. Acta Materialia, 2019, 166, 18-27.	7.9	27
25	Fast In Situ Nanotomography at ESRF. Microscopy and Microanalysis, 2018, 24, 450-451.	0.4	3
26	Localization, Characterization and Local Biokinetics of Tattoo Pigment Particles in Human Skin and Lymph Nodes by Means of Synchrotron-based Micro- and NanoXRF. Microscopy and Microanalysis, 2018, 24, 404-405.	0.4	0
27	4D Nano-Tomography for Fundamental Studies in Solidification of Aluminium-Based Alloys. Transactions of the Indian Institute of Metals, 2018, 71, 2765-2769.	1.5	0
28	Anisotropic sintering behavior of freeze-cast ceramics by optical dilatometry and discrete-element simulations. Acta Materialia, 2018, 155, 343-349.	7.9	24
29	Synchrotron-based μ-XRF mapping and μ-FTIR microscopy enable to look into the fate and effects of tattoo pigments in human skin. Scientific Reports, 2017, 7, 11395.	3.3	83
30	Coherently aligned nanoparticles within a biogenic single crystal: A biological prestressing strategy. Science, 2017, 358, 1294-1298.	12.6	97
31	Fast in situ 3D nanoimaging: a new tool for dynamic characterization in materials science. Materials Today, 2017, 20, 354-359.	14.2	86
32	Coupling in-situ X-ray micro- and nano-tomography and discrete element method for investigating high temperature sintering of metal and ceramic powders. EPJ Web of Conferences, 2017, 140, 13006.	0.3	1
33	Assessment of Ovarian Cancer Tumors Treated with Intraperitoneal Cisplatin Therapy by Nanoscopic X-ray Fluorescence Imaging. Scientific Reports, 2016, 6, 29999.	3.3	14
34	Nanoscopic tumor tissue distribution of platinum after intraperitoneal administration in a xenograft model of ovarian cancer. Journal of Pharmaceutical and Biomedical Analysis, 2016, 131, 256-262.	2.8	26
35	Visualization, quantification and coordination of Ag <sup>+</sup> ions released from silver nanoparticles in hepatocytes. Nanoscale, 2016, 8, 17012-17021.	5.6	68
36	Three-dimensional textural and quantitative analyses of orogenic gold at the nanoscale. Geology, 2016, 44, 739-742.	4.4	27

#	Article	IF	CITATIONS
37	ID16B: a hard X-ray nanoprobe beamline at the ESRF for nano-analysis. Journal of Synchrotron Radiation, 2016, 23, 344-352.	2.4	176
38	Fate of Ag-NPs in Sewage Sludge after Application on Agricultural Soils. Environmental Science & Technology, 2016, 50, 1759-1768.	10.0	151
39	Strength of hierarchically porous ceramics: Discrete simulations on X-ray nanotomography images. Scripta Materialia, 2016, 113, 250-253.	5.2	20
40	Innovative combination of spectroscopic techniques to reveal nanoparticle fate in a crop plant. Spectrochimica Acta, Part B: Atomic Spectroscopy, 2016, 119, 17-24.	2.9	43
41	X-ray micro Laue diffraction tomography analysis of a solid oxide fuel cell. Journal of Applied Crystallography, 2015, 48, 357-364.	4.5	14
42	X-ray nanotomography using near-field ptychography. Optics Express, 2015, 23, 12720.	3.4	34
43	Three dimensional analysis of Ce 0.9 Gd 0.1 O 1.95 –La 0.6 Sr 0.4 Co 0.2 Fe 0.8 O 3â^' δ oxygen electrode for solid oxide cells. Journal of the European Ceramic Society, 2015, 35, 4497-4505.	5.7	12
44	Degradation study by 3D reconstruction of a nickel–yttria stabilized zirconia cathode after high temperature steam electrolysis operation. Journal of Power Sources, 2014, 269, 927-936.	7.8	62
45	Quantitative microstructure characterization of a Ni–YSZ bi-layer coupled with simulated electrode polarisation. Journal of Power Sources, 2014, 256, 394-403.	7.8	48
46	Multi-scale 3D imaging of absorbing porous materials for solid oxide fuel cells. Journal of Materials Science, 2014, 49, 5626-5634.	3.7	28
47	X-Ray Tomography and Small-Angle Neutron Scattering Characterization of Nano-Composites: Static and In Situ Experiments. , 2014, , 1389-1393.		0
48	Degradation Study of the La <sub>0.6</sub> Sr <sub>0.4</sub> Co <sub>0.2</sub> Fe <sub>0.8</sub> O <sub>3</sub> Solid Oxide Electrolysis Cell (SOEC) Anode after High Temperature Electrolysis Operation. ECS Transactions, 2013, 57, 3177-3187.	0.5	15
49	Thermo-elastic properties of SOFC/SOEC electrode materials determined from three-dimensional microstructural reconstructions. International Journal of Hydrogen Energy, 2013, 38, 12379-12391.	7.1	41
50	3D phase mapping of solid oxide fuel cell YSZ/Ni cermet at the nanoscale by holographic X-ray nanotomography. Journal of Power Sources, 2013, 243, 841-849.	7.8	68
51	Synchrotron X-ray imaging applied to solar photovoltaic silicon. Journal of Physics: Conference Series, 2013, 425, 192019.	0.4	13
52	Highly resolved synchrotron-based investigations related to nuclear waste disposal. Materials Research Society Symposia Proceedings, 2012, 1444, 269.	0.1	4
53	Multiscale measurements of residual strains in a stabilized zirconia layer. Journal of Applied Crystallography, 2012, 45, 926-935.	4.5	8
54	Status of the hard X-ray microprobe beamline ID22 of the European Synchrotron Radiation Facility. Journal of Synchrotron Radiation, 2012, 19, 10-18.	2.4	95

#	Article	IF	CITATIONS
55	Synchrotron microanalysis techniques applied to potential photovoltaic materials. Journal of Synchrotron Radiation, 2012, 19, 521-524.	2.4	11
56	X-Ray Diffraction Determination of Macro and Micro Stresses in SOFC Electrolyte and Evolution with Redox Cycling of the Anode. Materials Science Forum, 2011, 681, 25-30.	0.3	4
57	Determination of global and local residual stresses in SOFC by X-ray diffraction. Nuclear Instruments & Methods in Physics Research B, 2010, 268, 282-286.	1.4	36
58	Structural and Chemical Variations in the Skeletal Segments of Coralline Red Algae Lead to Improved Crack Resistance. SSRN Electronic Journal, 0, , .	0.4	0
59	ID16B Beamline at the ESRF: a Nanoprobe for the Characterization of Nanomaterials and Nanodevices. , 0, , .		0